Journal of Renewable
Energy and Environment

Journal Homepage: www.jree.ir

Materials and Energy Research Center
MERC

Research Article

Effect of Solar Cell Materials on Energy Matrices of GISPVT System

Gopal Nath. Tiwari [a], Shikha Singh *[b], Yashwant Kumar Singh [c]

[a] BERS PUBLIC SCHOOL (BPS), P. O. Box: 221701, Jawahar Nagar (Margupur), Chilkhar, Ballia (UP), India.
[b] Department of Electrical Engineering, Shri Ramswaroop Memorial University (SRMU), P. O. Box: 225003, village Hadauri, Post Tindola, Barabanki, Uttar Pradesh, India.
[c] Lecturer, Government Polytechnic Alapur, Budaun, India.

PAPER INFO

Paper history:
Received: 21 November 2022
Revised: 14 March 2023
Accepted: 26 April 2023

Keywords:
Solar Cell Materials,
PV Module,
Energy Matrices,
Solar Energy

ABSTRACT

This paper presents an analytical expression for the temperatures of the plant, room air, and solar cell, as well as the electrical efficiency, for a photo-voltaic thermal (PVT) roof façade of a greenhouse integrated semi-transparent photovoltaic thermal (GiSPVT) system. The expression considers climatic variables such as solar intensity and ambient air temperature, as well as design parameters such as the area of the PV module, electrical efficiency under standard test conditions (STC), temperature coefficient, and various heat transfer coefficients. Using monthly numerical computations for different parameters in Indian climatic conditions, this study evaluates energy matrices such as energy payback time (EPBT), energy production factor (EPF), and life cycle conversion efficiency (LCCE) for various solar cell materials, including single-crystalline (c-Si), multi-crystalline (mc-Si), amorphous (a-Si), copper indium gallium diselenide (CIGS), and cadmium telluride (CdTe), with and without thermal exergy. Considering that the life span of greenhouse materials varies from 5-30 years for low cost, medium, and high-tech greenhouses, different solar cell materials are recommended for different life spans of GiSPVT. Therefore, this study recommends suitable solar cell materials for known greenhouse designs:

(a) The EPBT and (LCCE considering thermal exergy for c-Si/mc-Si range from approximately 3.5 to 4.5 years and 13 to 22%, respectively. Consequently, these values render crystalline silicon solar cells highly fitting for application in high-tech greenhouses with a comparable lifespan.

(b) For the CIGS, the EPBT is 1.17 years with an associated LCCE (including thermal exergy) of 16.44%. This establishes CIGS as particularly well-suited for deployment in cost-effective greenhouse environments

https://doi.org/10.30501/jree.2023.370499.1500

1. INTRODUCTION

Recently, the energy and food demand has been increasing significantly throughout the world due to uninterrupted population growth especially in developing and under-developing countries (increasing by more than 90 million per year) (as per internet source, Ref16). Simultaneously, the agricultural land is also declining due to fast growth of industrialization (as per internet source Ref2). Therefore, the demand for energy and food security per capita has increased significantly in recent years. In order to meet these demand/requirements, the existing available land must be accessible to increase agricultural yield, particularly vegetables, and electrical power generation on a yearly basis. One of the concepts introduced for remote rural areas is the greenhouse integrated semi-transparent photovoltaic (GiSPVT) system (Yadav et. al., 2022 and Tiwari et. al., 2022), which combines vegetable production and electricity generation. The GiSPVT can be used in barren lands to increase productivity in various ways (Tiwari and Tiwari, 2021 and Deo et.al., 2017). The mentioned system is a self-sustaining system that is not only environmentally-friendly but adaptable to climate change, especially to cold climates. In addition, the electrical power generated by the system can be used for cooling a greenhouse under any hot climatic conditions. Tiwari and Tiwari, 2021 implemented such a unit in Jawahar Nagar (Magupur), Chilkahar-22 17 01, Ballia (UP), India on barren land with an effective area of 80×120 square feet and a capacity of 30kWp. They utilized a single crystalline silicon solar cell with varying packing factors for the semi-transparent PV module. The system used a c-Si based semi-transparent PV module as a roof façade, due to its longer lifespan of 30 years with a reinforced concrete-cement (RCC) structure, making it a high-tech greenhouse.

Many attempts have been made so far to increase the electrical efficiency, stability, and service life of a solar cell to make the solar photo-voltaic thermal (PVT) system more economical (Durish et. al., 2007, Virtuani et. al., 2010, Tiwari and Mishra, 2011 and Evans, 1981). Thermal coefficient is one of the sensitive parameters that affects the electrical performance of a PV module. As reported in the literature, researchers have managed to compile electrical efficiency, expected life, specific

*Corresponding Author's Email: ishikha.singh@gmail.com (S. Singh)
URL: https://www.jree.ir/article_171080.html

Please cite this article as: Tiwari, G. N., Singh, S. & Singh, Y. K. (2024). Effect of Solar Cell Materials on Energy Matrices of GISPVT System, *Journal of Renewable Energy and Environment (JREE)*, 11(1), 65-73. https://doi.org/10.30501/jree.2023.370499.1500.

energy densities, and thermal coefficients of different solar cell materials, namely single-crystalline (c-Si), multi-crystalline (mc-Si) and amorphous (a-Si), copper indium gallium diselenide (CIGS), and Cadmium Telluride (CdTe) (Rathore et. al, 2019, Murali et. al., 2021, Karthicka et. al., 2018, Mishra and Tiwari, 2013 and Agrawal and Tiwari, 2013). It is also known that the integration of semitransparent photovoltaic (PV) module is most suitable for greenhouses of uneven type. The construction material used for greenhouses has different life spans, varying from 5 to 30 years (Tiwari, 2003).

Due to different life spans of greenhouse construction, a suitable solar cell material is required for a given design of a greenhouse that matches the life of greenhouses based on energy matrices. Therefore, there is a strong need to study the effect of different solar cell materials of solar cell on the performance of GiSPVT system in terms of energy matrices.

To evaluate the energy matrices of the GiSPVT system with and without thermal exergy, the present study is carried out. The numerical computations for different solar cell materials in the GiSPVT system are performed using average temperature coefficients. The analytical expression for electrical efficiency, derived in this study in terms of the thermal coefficient of the PV module, is utilized to calculate the monthly variation of electrical power produced from the roof face of the GiSPVT system. The monthly average solar radiation and ambient air temperature for Indian climatic conditions are used in the computation. Based on monthly performance, annual electrical power used to calculate energy matrices has been evaluated. On the basis of numerical computation, it has been observed that (i) c-Si base PV module is more practical and economical from energy point of view for a high-tech greenhouse than other solar cell materials and (ii) there is not significant variation in energy matrices by considering thermal exergy. Further, experimental validation of hourly variation of the plant, the room air, and the solar cell temperatures has been carried out using the present thermal model of GiSPVT for a typical day.

2. OPERATING PRINCIPLE OF GREENHOUSE INTEGRATED SEMI-TRANSPARENT PHOTO-VOLTAIC THERMAL (GISPVT) SYSTEM

Figure 1 shows the cross-sectional view of an uneven greenhouse integrated semi-transparent photo-voltaic thermal (GiSPVT) system, which has been used for the present analysis. The incident solar radiation on the roof façade is directly transmitted through the non-packing area of a semi-transparent PV module inside the greenhouse $\left[\tau_g^2(1-\beta)A_{RS}I(t)\right]$, which is a direct gain. Further, the incident solar radiation falling on the packing area of a semi-transparent PV module after transmission from the top glass cover of PV module $\left[\alpha_c\tau_g\beta A_{RS}I(t)\right]$ is partially converted into DC power $\left[\eta_0\tau_g\beta A_{RS}I(t)\right]$ and the remaining is used to heat the solar cell of PV module, hence an increase in its temperature. After the increase in the temperature of the solar cell of PV module, there are indirect top $\left[U_{t,ca}(T_c-T_a)A_{RS}\right]$ and bottom losses $\left[U_{b,cr}(T_c-T_r)A_{RS}\right]$ to ambient and inside greenhouse through conduction and convection, as shown in Figures. 2 and 3, respectively. The solar radiation that enters the GiSPVT room directly is utilized for photosynthesis or for heating the plants and the air inside the greenhouse. On the other hand, the indirect gain to the greenhouse room is only utilized for thermal heating of the greenhouse air. The electrical efficiency of the solar cell in the PV module will be at its maximum when there is a maximum thermal energy loss from the solar cell to both the ambient and greenhouse air, which is due to the low operating temperature range of the solar cell. Thermal resistance and thermal circuit diagram of the GiSPVT system are shown in Figures 2 and 3, respectively. The design parameters and various heat transfer coefficients are given in Table 1.

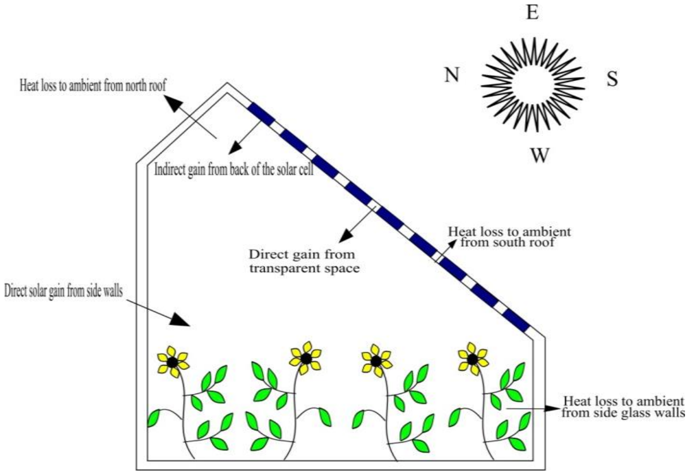

Figure 1. Schematic diagram of the greenhouse integrated semi-transparent photo-voltaic thermal (GiSPVT) system

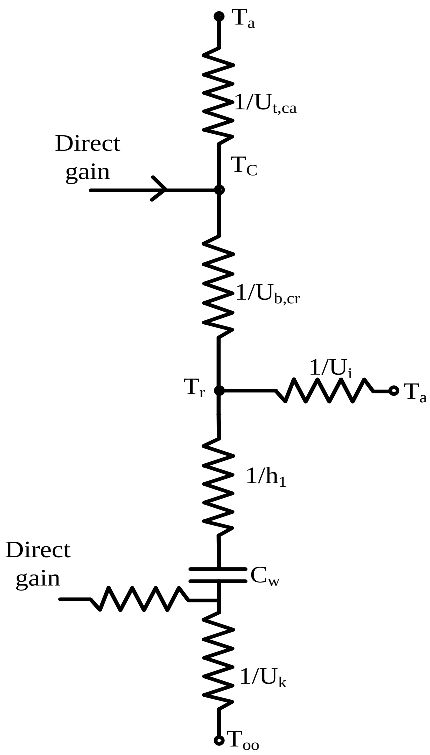

Figure 2. Thermal resistance diagram of GiSPVT

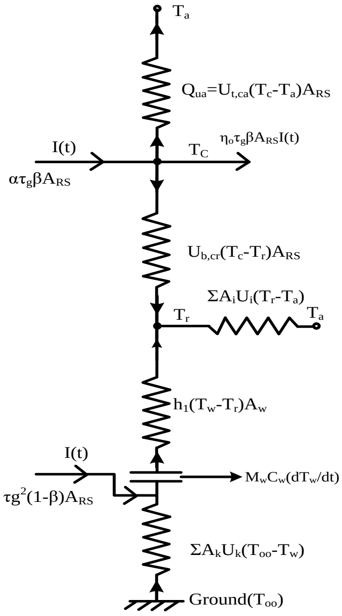

Figure 3 Thermal circuit diagram of the GiSPVT system

Table 1. Design parameters of GiSPVT system (Tiwari et al., 2022)

Parameters	Numerical values	Parameters	Numerical values
A_m	0.71m^2	No of PV module	168
A_W(glass A_E = wall)	37.12	U_{ra1}	3.5084 W/m^2°C
A_SA_N =	44.6227	$U_{t,ca}$	9.1794 W/m^2°C
A_{RN}	83.9785m^2	α_c	0.9
A_{RS}	245.05m^2	β	0.22, 0.5, 0.8
$A_{WPE} = A_{WPW}$	0.1219	τ_g	0.95
A_{WPB} = Aw	297.87m^2	η_0	0.15
C_w	4192 J/kg°C	$(\alpha\tau)_{eff}$	0.2179
V_w	(100-535)m^3	$(\alpha\tau)_{meff}$	85.9006
PF_1	0.3822	γ	0.98
PF_2	0.7805	T_{00}	25°C
$(UA)_{wa}$	1375.5	$U_{b,cr}$	5.6789 W/m^2°C
U_i	3.5 W/m^2°C	U_k	1-3 W/m^2°C

3. THERMAL AND ELECTRICAL ANALYSIS OF THE SYSTEM

The following assumptions are considered to develop energy balance equation for each component of the GiSPVT system:

(i) The analysis has been carried out in a quasi-steady state condition.

(ii) No electrical losses have been considered between two solar cells of PV module due to low electrical resistance of copper material.

(iii) Ethyl Vinyl Acetate (EVA) has about 100% transmittivity.

(iv) The heat capacities (M_pC_p) of the plant and the water (M_wC_w) are considered the same due to maximum holding of water in the plants.

(v) Across thickness of conducting, insulating and air materials, there is no temperature gradient.

(vi) Heat capacity of each material of GiSPVT is negligible, except the heat capacity of plant.

(vii) All walls are covered by movable insulating curtains.

(viii) The inside ground temperature is assumed to be equal to ambient temperature, i.e., $T_{00} \cong \overline{T_a}$.

Based on the above assumptions and following Figures. 2 and 3, the basic energy balance for each component of uneven GiSPVT is written as follows:

(a) For semi-transparent south PV roof

$$\alpha_c\tau_g\beta A_{RS}I(t) = U_{t,ca}(T_c - T_a)A_{RS} + U_{b,cr}(T_c - T_r)A_{RS} + \eta_0\tau_g\beta A_{RS}I(t) \quad (1)$$

The values of electrical efficiency under standard test condition (STC), energy density, temperature coefficient, and embodied energy for different solar cell materials are given in Table 2.

(b) For GiSPVT room air

$$U_{b,cr}(T_c - T_r)A_{RS} + h_1(T_p - T_r)A_P = \sum_{i=1}^{5} A_i\, U_i(T_r - T_a) \quad (2)$$

(c) For plant inside GiSPVT

$$\sum_{k=1}^{5} A_k\, U_k(T_{00} - T_w) + \tau_g{}^2(1-\beta)A_{RS}I(t) + \tau_g\sum_{j=1}^{3} A_j\, I_j = M_pC_p\frac{dT_p}{dt} + h_1(T_p - T_r)A_P \quad (3)$$

where $\tau_g\sum_{j=1}^{3} A_j\, I_j$=0. All solar radiation exposed walls are either opaque walls of un-even GiSPVT or insulated glass walls, and the north roof takes zero value as per last assumption vii.

Following (Tiwari et al., 2022) and some algebraic simplification, the solution to Eq. 3 can be obtained below:

$$T_p = \left\{\frac{\left[\{\tau_g{}^2(1-\beta)+PF_2(\alpha\tau)_{eff}\}A_{RS}\overline{I(t)}+\tau_g\sum_{j=1}^{3}A_j\overline{I_J}\right]}{\left[(UA)_{wa}+\sum_{k=1}^{5}A_kU_k\right]} + \overline{T_a}\right\}(1 - e^{-at}) + T_{p0}e^{-at} \quad (4)$$

where T_{p0} is the initial plant temperature at t = 0, $a = \frac{\left[(UA)_{wa}+\sum_{k=1}^{5}A_kU_k\right]}{M_wC_w}$ and

$$PF_2 = \frac{h_1A_w}{h_1A_w + U_{ra1}A_{RS} + \sum_{i=1}^{5}A_iU_i}$$

Now, the average water temperature can be determined as follows:

$$\bar{T}_p = \frac{1}{t}\int_0^t T_w\, dt = \left\{\frac{\left[\{\tau_g{}^2(1-\beta)+PF_2(\alpha\tau)_{eff}\}A_{RS}\overline{I(t)}+\tau_g\sum_{j=1}^{3}A_j\overline{I_J}\right]}{\left[(UA)_{wa}+\sum_{k=1}^{5}A_kU_k\right]} + \overline{T_a}\right\}\left(1 - \frac{1-e^{-at}}{at}\right) + T_{p0} \quad (5)$$

After evaluating hourly variation of $\bar{T}_p$ from Eq. 5 from a given design and climatic parameters, the hourly average variation of room air and solar cell temperatures is obtained using the following equations as:

$$\overline{T_r} = \frac{(\alpha\tau)_{eff}A_{RS}\overline{I(t)}+\left[U_{ra1}A_{RS}\overline{T_a}+h1A_PT_P+\sum_{i=1}^{5}A_iU_i\overline{T_a}\right]}{\left[U_{ra1}A_{RS}+h1A_P+\sum_{i=1}^{5}A_iU_i\right]} = \frac{(\alpha\tau)_{eff}A_{RS}\overline{I(t)}}{\left[U_{ra1}A_{RS}+h1A_P+\sum_{i=1}^{5}A_iU_i\right]} + \frac{\left[U_{ra1}A_{RS}+\sum_{i=1}^{5}A_iU_i\right]}{\left[U_{ra1}A_{RS}+h1A_P+\sum_{i=1}^{5}A_iU_i\right]}\overline{T_a} + \frac{h1A_P}{\left[U_{ra1}A_{RS}+h1A_P+\sum_{i=1}^{5}A_iU_i\right]}\bar{T}_p \quad (6)$$

and

$$\overline{T_c} = \frac{\tau_g\beta(\alpha_c-\eta_0)\overline{I(t)}+U_{t,ca}\overline{T_a}+U_{b,cr}\overline{T_r}}{U_{b,cr}+U_{t,ca}} = \frac{\tau_g\beta(\alpha_c-\eta_0)\overline{I(t)}+U_{t,ca}\overline{T_a}}{U_{b,cr}+U_{t,ca}} + \frac{U_{b,cr}}{U_{b,cr}+U_{t,ca}}\overline{T_r} \quad (7)$$

Equations 4-7 are applicable to most of blue sky clear climatic conditions and it is used to evaluate (a) monthly average variation of plant, solar cell, and room air temperatures in the present study and (b) daily hourly variation of plant, solar cell, and room air temperatures for given hourly solar intensity and ambient air temperature for experimental validation.

Substituting Eq. 6 into Eq. 7, we can:

$$\overline{T_c} = \frac{\tau_g\beta(\alpha_c-\eta_0)\overline{I(t)}+U_{t,ca}\overline{T_a}}{U_{b,cr}+U_{t,ca}} + \frac{U_{b,cr}}{U_{b,cr}+U_{t,ca}}\left[\frac{(\alpha\tau)_{eff}A_{RS}\overline{I(t)}}{[U_{ra1}A_{RS}+h1A_P+\sum_{i=1}^{5}A_iU_i]} + \frac{[U_{ra1}A_{RS}+\sum_{i=1}^{5}A_iU_i]}{[U_{ra1}A_{RS}+h1A_P+\sum_{i=1}^{5}A_iU_i]}\overline{T_a} + \frac{h1A_P}{[U_{ra1}A_{RS}+h1A_P+\sum_{i=1}^{5}A_iU_i]}\overline{T_p}\right]$$

or,

$$\overline{T_c} = \frac{\tau_g\beta(\alpha_c-\eta_0)\overline{I(t)}+U_{t,ca}\overline{T_a}}{U_{b,cr}+U_{t,ca}} + \frac{U_{b,cr}}{U_{b,cr}+U_{t,ca}} \times \frac{(\alpha\tau)_{eff}A_{RS}\overline{I(t)}}{[U_{ra1}A_{RS}+h1A_P+\sum_{i=1}^{5}A_iU_i]} + \frac{U_{b,cr}}{U_{b,cr}+U_{t,ca}} \times \frac{[U_{ra1}A_{RS}+\sum_{i=1}^{5}A_iU_i]}{[U_{ra1}A_{RS}+h1A_P+\sum_{i=1}^{5}A_iU_i]}\overline{T_a} + \frac{U_{b,cr}}{U_{b,cr}+U_{t,ca}} \times \frac{h1A_P}{[U_{ra1}A_{RS}+h1A_P+\sum_{i=1}^{5}A_iU_i]}\overline{T_p} \quad (8)$$

Now, substituting an expression for $\overline{T}_w$ from Eq. 5 into Eq. 8, one gets

$$\overline{T_c} = \frac{\tau_g\beta(\alpha_c-\eta_0)\overline{I(t)}+U_{t,ca}\overline{T_a}}{U_{b,cr}+U_{t,ca}} + \frac{U_{b,cr}}{U_{b,cr}+U_{t,ca}} \times \frac{(\alpha\tau)_{eff}A_{RS}\overline{I(t)}}{[U_{ra1}A_{RS}+h1A_P+\sum_{i=1}^{5}A_iU_i]} + \frac{U_{b,cr}}{U_{b,cr}+U_{t,ca}} \times \frac{[U_{ra1}A_{RS}+\sum_{i=1}^{5}A_iU_i]}{[U_{ra1}A_{RS}+h1A_P+\sum_{i=1}^{5}A_iU_i]}\overline{T_a} + \frac{U_{b,cr}}{U_{b,cr}+U_{t,ca}} \times \frac{h1A_P}{[U_{ra1}A_{RS}+h1A_P+\sum_{i=1}^{5}A_iU_i]}\left[\left\{\frac{[\{\tau_g{}^2(1-\beta)+PF_2(\alpha\tau)_{eff}\}A_{RS}\overline{I(t)}+\tau_g\sum_{j=1}^{3}A_j\overline{I_j}]}{[(UA)_{wa}+\sum_{k=1}^{5}A_kU_k]} + \overline{T_a}\right\}\left(1-\frac{1-e^{-at}}{at}\right) + T_{p0}\frac{1-e^{-at}}{at}\right] \quad (9)$$

The above thermal model for GiSPVT room air and solar cell temperature for a typical day of Ballia (UP), India has been validated experimentally (Tiwari, et al, 2022).

4. ELECTRICAL POWER OF GISPVT

For known analytical expression of monthly average solar cell temperature $(\overline{T_c}), Eq. 8$, an analytical expression of monthly average instantaneous electrical efficiency of PV module $(\bar{\eta}_{mi}), Evans$ (1981), of the un-even GiSPVT can be obtained as follows:

$$\bar{\eta}_{mi} = \tau_g\eta_0\left[1-\beta_0\left(\frac{\tau_g\beta(\alpha_c-\eta_0)\overline{I(t)}+U_{t,ca}\overline{T_a}}{U_{b,cr}+U_{t,ca}} + \frac{U_{b,cr}}{U_{b,cr}+U_{t,ca}} \times \frac{(\alpha\tau)_{eff}A_{RS}\overline{I(t)}}{[U_{ra1}A_{RS}+h1A_P+\sum_{i=1}^{5}A_iU_i]} + \frac{U_{b,cr}}{U_{b,cr}+U_{t,ca}} \times \frac{[U_{ra1}A_{RS}+\sum_{i=1}^{5}A_iU_i]}{[U_{ra1}A_{RS}+h1A_P+\sum_{i=1}^{5}A_iU_i]}\overline{T_a} + \frac{U_{b,cr}}{U_{b,cr}+U_{t,ca}} \times \frac{h1A_P}{[U_{ra1}A_{RS}+h1A_P+\sum_{i=1}^{5}A_iU_i]}\left[\left\{\frac{[\{\tau_g{}^2(1-\beta)+PF_2(\alpha\tau)_{eff}\}A_{RS}\overline{I(t)}+\tau_g\sum_{j=1}^{3}A_j\overline{I_j}]}{[(UA)_{wa}+\sum_{k=1}^{5}A_kU_k]} + \overline{T_a}\right\}\left(1-\frac{1-e^{-at}}{at}\right) + T_{w0}\frac{1-e^{-at}}{at}\right] - 25\right)\right] \quad (10)$$

Eq. 10 can be used to determine the average monthly PV module efficiency for the numerical value of η_0 and β_0 for different solar cell materials, as given in Table 2.

Table 2 Specifications of various silicon and non-silicon-based PV modules (Durisch et al., 2007; Virtuani et al. 2010; Tiwari and Mishra, 2007)

Different Solar cell materials	PV module efficiency η_{mo}(%)	Expected life n_{PV} (Yrs)	Specific energy density E_{in} (kWh m^{-2})	(E_{in}) of PV module, A_m=0.71 m^2 (kWh)	Average temp. coefficient β ($^oC^{-1}$)
c-Si (Single-crystalline)	16	30	1190	8449	0.00535
mc-Si (Multi-crystalline silicon)	14	30	910	646.1	0.00425
nc-Si (Nano-crystalline -Silicon)	12	25	610	433.1	0.0036
a-Si (Amorphous silicon)	6	20	378	268.38	0.00115
CdTe (Cadmium Telluride)	8	15	266	188.86	0.00205
CIGS (Copper indium gallium selenide)	10	5	24.5	17.395	0.00335

4.1.1 Monthly Average Electrical Output

By using the monthly average value of PV module electrical efficiency $(\bar{\eta}_{mi})$ obtained from Eq. 10 for monthly electrical energy, $E_{monthly}$ in kWh is given as

$$E_{monthly}(kWh) = \frac{\eta_{mi}\times I(t)\times A_m\times \text{Number of PV module}\times N\times \text{number of days in month}}{1000} \quad (11)$$

where N is the number of sunshine hours in a day and varies from January to December for a given location.

4.1.2 The Yearly Electrical Output

Yearly electrical output of monthly electrical energy from January to December can be obtained by

$$E_{yearly}(kWh) = \sum_{k=1}^{12} E_{monthly,k} \quad (12)$$

4.2 Thermal Energy of GiSPVT

The average monthly thermal energy can be obtained as follows:

$$Q_{u,monthly,th}(KWh) = \frac{M_wC_w(T_{w,monthly}-T_a)}{1000\times 3600} \times 24 \times \text{numberof days in a given month} \quad (13a)$$

where $T_{w,monthly}$ is monthly variation of water temperature obtained from Eq. 5.

The average monthly thermal exergy, $Q_{u,monthly,th-ex}$, can be determined using Eq. 13a as follows:

$$Q_{u,monthly,th-ex}(KWh) = \frac{M_wC_w(T_{w,monthly}-T_a)}{1000\times 3600} \times 24 \times \text{number of days in month} \quad (13b)$$

The average yearly thermal exergy, $Q_{u,monthly,th}(KWh)$, is given by

$$Q_{u,monthly,th}(KWh) = \frac{M_p C_p (T_{w,monthly} - T_a)}{1000\times3600} \times 24 \times \text{number of days in a given month} \quad (13c)$$

The average yearly thermal exergy, $Q_{u,yearly,th}$, is given by

$$Q_{u,yearly,th}(KWh) = \frac{M_p C_p \times 24\times365}{1000\times3600}\left[(T_{w,max} - T_{w,min}) - (\overline{T_a} + 273) ln\frac{T_{w,max}+273}{T_{w,min}+273}\right] \quad (14)$$

where $T_{w,max}$ and $T_{w,min}$ can be obtained from monthly variation from analytical expression o water temperature (T_w) using Eq. 5 for the given climatic and design parameters.

Total yearly exergy of GiSPVT can be respectively written using Eqs. 11 and 16b as follows:

$$Ex_{T,yearly} = E_{yearly}(kWh) + Q_{u,yearly,th}(KWh \quad (15)$$

5. ENERGY MATRICES

The energy payback time, the energy production factor, and the life cycle conversion efficiency are three main energy matrices. In the following subsection, without thermal exergy and with thermal exergy, these matrices have been assessed for various solar cell materials

5.1 Energy Payback Time (EPBT)

(a) Without Thermal Exergy

Now, the total embodied energy ($E_{in,T}$) of semitransparent roof of GiSPVT can be evaluated as

$$E_{in,T} = \text{The number of semitransparent PV modules in south roof} \times \text{an area of one PV module } (m^2) \times \text{embodied energy } E_{in}(kWh) \quad (16)$$

Here, the embodied energy for a given design of GiSPVT system is constant for different solar cell materials.

The embodied energy, $E_{in}(kWh)$, for the PV module of 0.71 m^2 for different solar cell materials is given in Table 2.

Then energy payback time (EPBT) of the GiSPVT system is calculated as follows:

$$EPBT = \frac{E_{in,T}}{E_{yearly}} \gg 1 \quad (17)$$

The numerical values of E_{yearly} and $E_{in,T}$ can be considered for different solar cell materials using Eqs. 11 and 15, respectively. In this case, we will analyze the GiSPVT system without thermal exergy. If EPBT is much less than the expected life of the semi-transparent PV roof system, then thePV system will be considered economical; otherwise, it is rejected.

5.2 Energy Production Factor (EPF)

The energy production factor (EPF) is the whole life of GiSPVT system which depends on annual electrical energy $[E_{yearly}]$, life of PV system, and embodied energy ($E_{in,T}$) and it is defined as follows:

$$EPF = \frac{E_{yearly}\times \text{Life of PV system}}{E_{in,T}} > 1 \quad (18)$$

Further, the numerical value of EPF should be as maximum as possible along with minimum energy payback time (EPBT).

5.3 Life Cycle Conversion Efficiency (LCCE)

The life cycle conversion efficiency (LCCE) depends on annual electrical energy $[E_{yearly}]$, life of PV system, and embodied energy ($E_{in,T}$) along with annual solar radiation and it is defined as follows:

$$LCCE = \frac{E_{yearly}\times \text{Life of PV system} - E_{in,T}}{\text{Yearly solar radiation}\times \text{Life of PV system}} < 1 \quad (19)$$

Here,

$$\text{Yearly solar radiation on roof (kWh)} = \frac{\text{number of PV module}\times\text{area of PV module} \times\sum_{j=1}^{12} I_j \times 11hr}{1000} \quad (20)$$

It is to be seen that among all the cases considered for different solar cell materials, the GiSPVT system will be economically viable from an energy standpoint if the following criteria are met:

- EPBT should be minimized;
- EPF should be maximized;
- LCCE should be maximized.

(a) With Thermal Exergy

In this case, a yearly electrical energy in Eq. 12 is replaced by total exergy, $Ex_{T,yearly}$, in Eq. 15. Thus, the above conditions should be met.

6. METHODOLOGY TO ESTIMATE THE ENERGY MATRICES OF GISPVT SYSTEM

As shown in the flow chart in Figure 4, the numerical computation is adopted as follows:

Step 1: Equations 9-12 are directly used to compute monthly average (i) solar cell temperature, $\overline{T}_c$, (ii) instantaneous PV module electrical efficiency, η_{mi}, (iii) the electrical energy, $E_{monthly}$, and (iv) yearly electrical energy, E_{yearly}, based on the data given in Table 1 and Figure 5. The results are summarized in Figures 6-9.

Step 2: Equation 5 is employed to compute the monthly average water temperature, $[\overline{T}_w]$, Figure 6.

Step 3: After determining the monthly average water temperature $[\overline{T}_w]$ using Eq.5, Eqs. 13-14 are used to evaluate the monthly thermal energy, $Q_{u,monthly,th}$, the monthly thermal exergy, $Q_{u,monthly,th-ex}$, and the yearly exergy, $Q_{u,yearly,th}$.

Step 4: Equation 6 is used to compute the average monthly GiSPVT room air based on $[\overline{T}_w]$ data given in Step 2, Figure 13.

Step 5: After determining $E_{yearly}(kWh)$ in Step 1 and $Q_{u,yearly,th}(KWh)$ in Step 3, the total yearly exergy($Ex_{T,yearly}$) can be evaluated through Eq. 15, Figure 14.

Step 6: Equations 17-19 are utilized to compute energy matrices of the GiSPVT system based on the data given in Steps 1-4, Table 3.

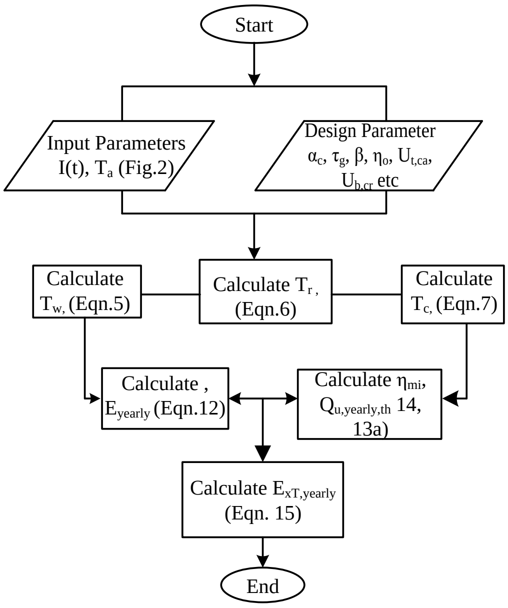

Figure 4. Flowchart of the GiSPVT system

7. RESULTS AND DISCUSSION

Numerical computations were conducted using Matlab based on the methodology outlined in Section 6, and using the design parameters listed in Table 1 and climatic parameters shown in Figure 5. The observed decreasing trend in monthly solar radiation from May to December can be attributed to the changing weather conditions from summer to rainy and then winter conditions. During these periods, there is an intermittent cloudy condition and there is variation in sunshine hours. The average solar cell temperature of each material, as shown in Figure 6, indicates that there is not much difference between temperatures of each individual solar cell. It may be due to the negligible heat capacity of solar cell material (assumption vi). The solar cell temperature is maximum in summer (92°C) and minimum in winter (30°C) as per expectation. Further, the instantaneous electrical efficiency of the solar cell is minimum in summer and maximum in winter as per conclusion given by various authors (Figure 7). However, Figure 8 shows that the average monthly variation of electrical energy is maximum for c-Si solar cells and minimum for CdTe solar cells. These decreasing trends result from decrease in electrical efficiency of solar cell materials, as given in Table 2. It should be noted that there is a decrease in monthly electrical energy during the months between March and May, and August and September due to changes in the solar radiation values, as shown in Figure 5 for partially cloudy conditions during these months. However, the yearly electrical energy for c-Si and a-Si solar cells is maximum (2000 kWh) and minimum (750 kWh), respectively, as shown in Figure 9.

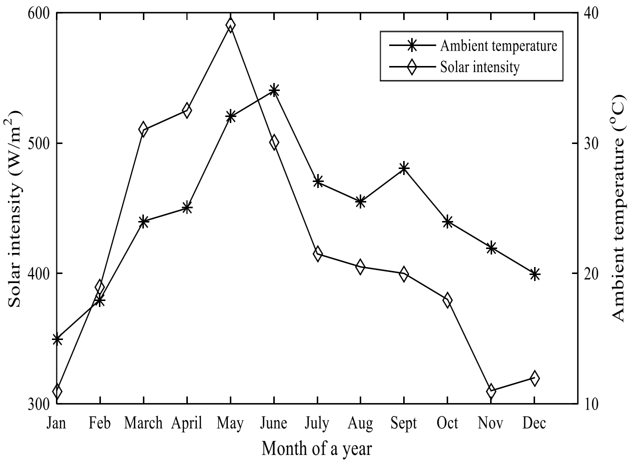

Figure 5. Monthly average variation of solar radiation (W/m^2) and ambient temperature for a composite Indian climatic condition

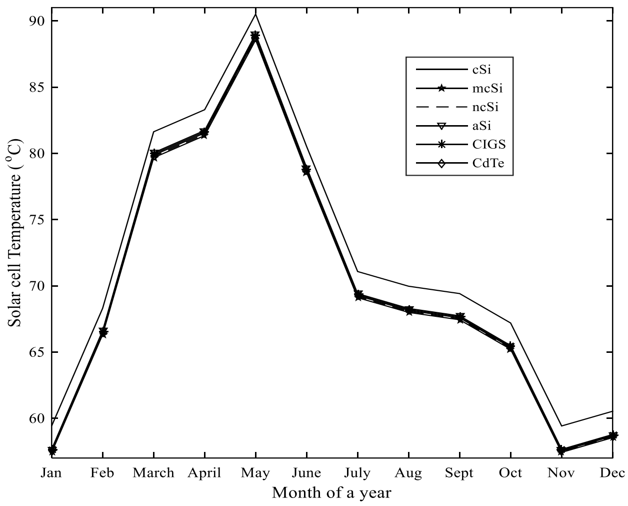

Figure 6. Average monthly variation of solar cell temperature for different solar cell materials

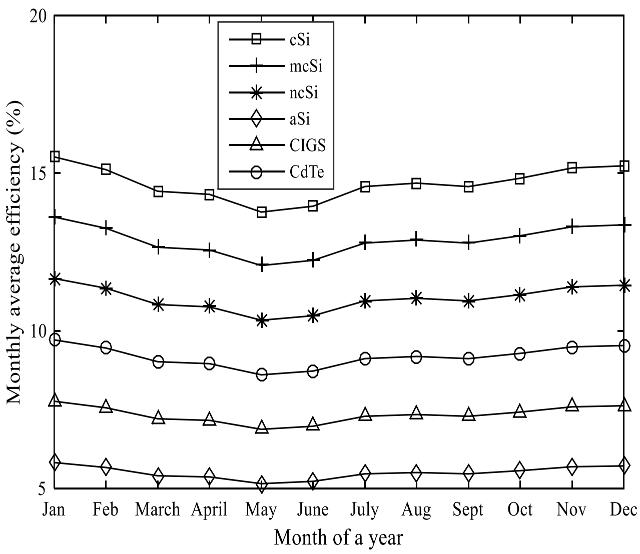

Figure 7. Average monthly variation of electrical efficiency of the solar cell for different solar cell materials

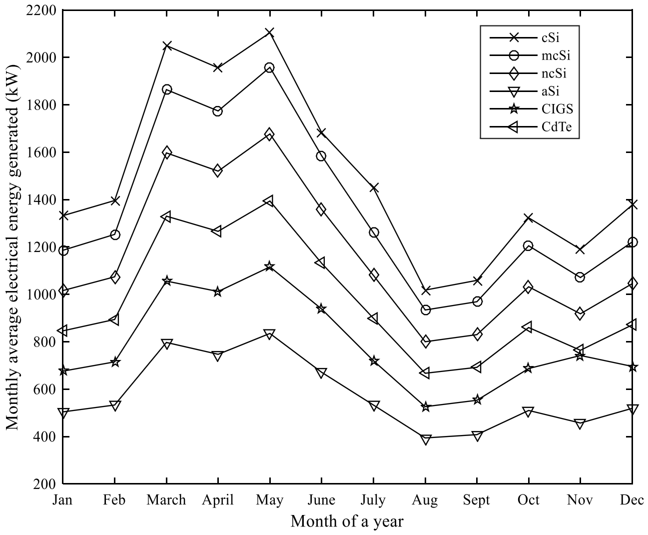

Figure 8. Average monthly variation of electrical energy of solar cell for different solar cell materials

According to Figure 10, the average monthly variation of GiSPVT water/plant temperature is similar for most solar cell materials, with only the crystalline silicon (c-Si) cells showing slightly higher temperatures. The temperature is maximum (46.5°C) in May due to longer clear days and sunshine hours. Further, the monthly variation of thermal energy based on the first law of thermodynamics is shown in Figure 11 and the monthly exergy based on the second law of thermodynamics is shown in Figure 12. There is a change in variation due to the destruction that takes place in the second law of thermodynamics, unlike the first law of thermodynamics.

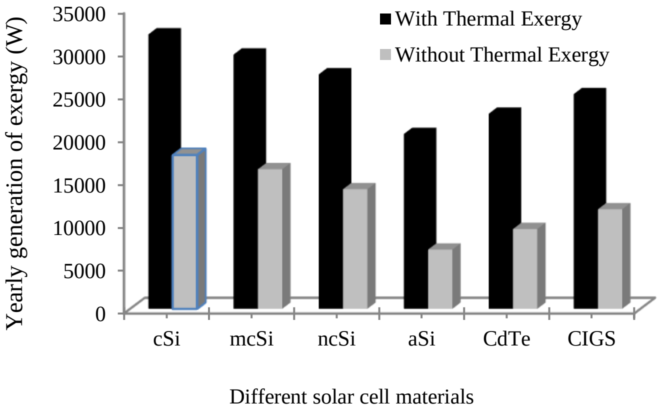

Figure 9. Yearly electrical energy of solar cell for different solar cell materials

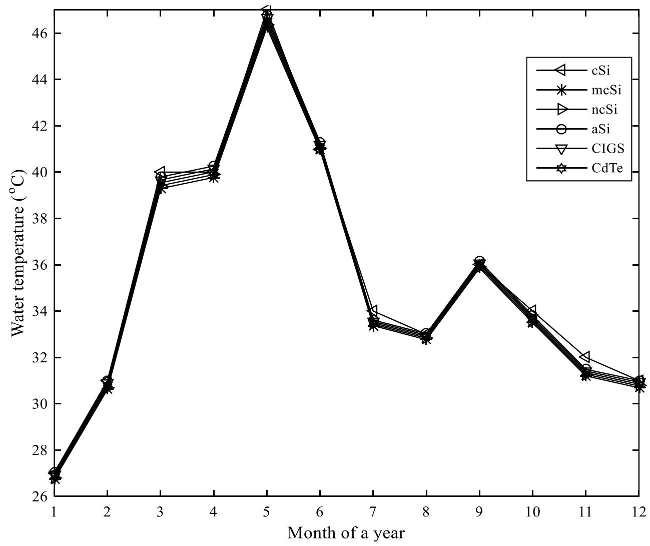

Figure 10. An average monthly variation of GiSPVT water temperature for different solar cell materials

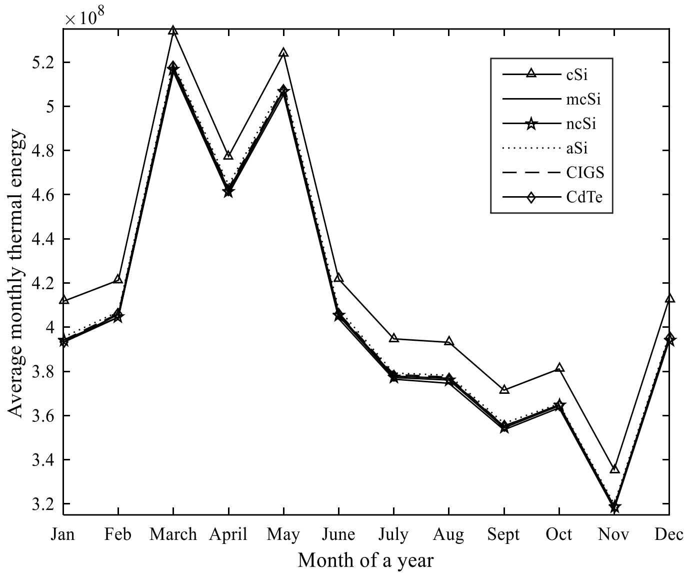

Figure 11. An average monthly variation of thermal energy of GiSPVT for different solar cell materials

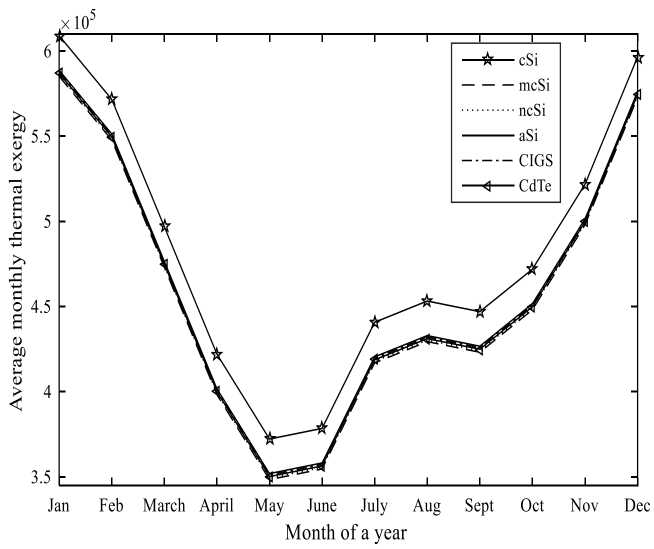

Figure 12. An average monthly variation of thermal exergy of GiSPVT for different solar cell materials

An average monthly variation of GiSPVT room air temperature for different solar cell materials is shown in Figure 13, which is lower than the solar cell temperature (Figure 13) and higher than water temperature (Figure 10). The results are consistent with our expectation, with similar trends observed in Figures 13 and 14.

Equation 15 is used to evaluate the total exergy, which includes yearly electrical energy and thermal exergy of GiSPVT system for different solar cell materials, as shown in Figure 14. It can be seen that the total exergy for c-Si solar cell is maximum and minimum for mc-Si solar cell. Both c-Si solar cell and mc-Si solar cell are most suitable for high-tech uneven-type greenhouse construction.

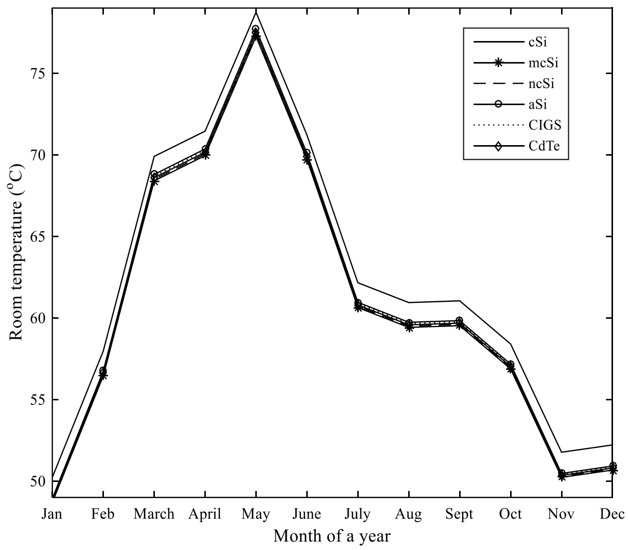

Figure 13. An average monthly variation of GiSPVT room air temperature for different solar cell materials

Energy matrices namely energy payback time (EPBT), energy production factor (EPF), and life cycle conversion efficiency (LCCE) are calculated using Eqs. 17-19 with and without thermal exergy. The results for yearly exergy with and without thermal exergy obtained in Figures. 5-14 are used and the results are obtained for energy matrices and given in Table 3. In addition to energy matrices, we have also evaluated the difference between the life of a semitransparent PV module and its energy payback time (EPBT). This is very important in making decisions about economic viability of a PV module for each material. Here, one can observe that the CIGS solar cell has a minimum energy payback time of 2.52 years; however, the life of CIGS solar cell is 5 years. This means that it can work more than 2.48 years in addition to its EPBT of 2.52 years. This indicates that the CIGS PV module should be replaced every five years. Therefore, the CIGS PV module is most suitable for low-cost greenhouses. Although c-Si and mc-Si solar cell materials have the same lifespan of 30 years, the difference between their energy payback time (EPBT) and the lifespan of the PV module is 22.04 and 23.33 years, respectively. Furthermore, since the mc-Si solar cell has a shorter energy payback time of 6.67 years, it is preferred over all other solar cell materials for the manufacturing of PV modules and is even more preferable for high-tech greenhouses. As can be implied, There is an improvement of 3 years in the difference between the life of the PV module and the energy payback time by considering thermal exergy in evaluating energy matrices.

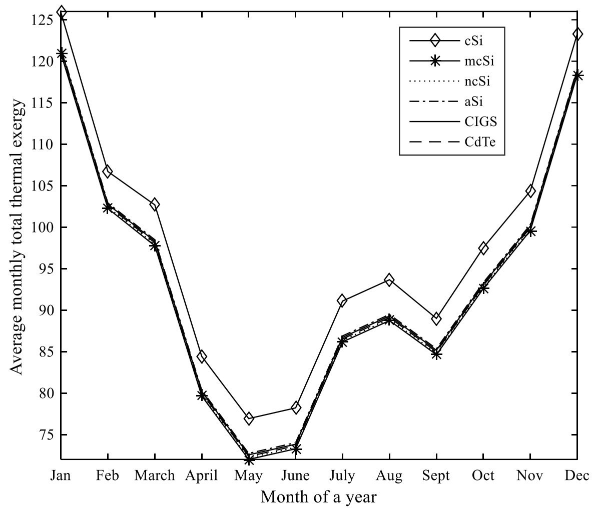

Figure 14. An average monthly variation of total exergy of GiSPVT for different solar cell materials

8. EXPERIMENTAL VALIDATION

Equations 5-7 are utilized to compute hourly plant, room air, and solar cell temperatures for design parameters given in Table 2 and the hourly data of solar radiation and ambient air temperature determined by (Tiwari et al., 2021). The results are summarized in Figure 15. It is quite clear that the hourly solar cell temperature is higher than GiSPVT room air and the plant temperatures, as expected. Further, the results of Figure 15 are consistent with the results reported in Figures 6, 10, and 13 for monthly variation.

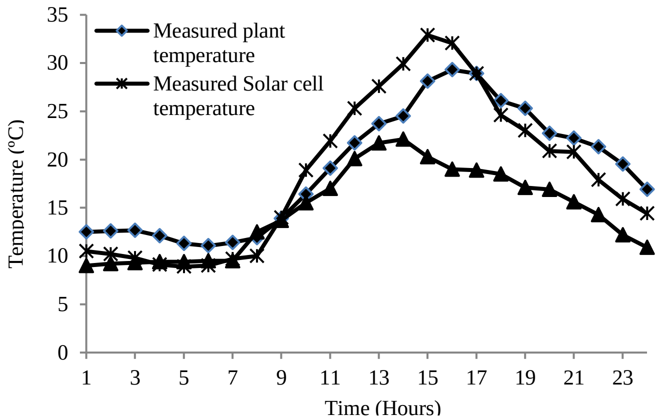

Figure 15. Experimental observation of hourly variation of plant, room air, and solar cell temperatures by the present model for each temperature adopted from (Tiwari,.et al, 2022)

9. CONCLUSIONS AND RECOMMENDATIONS

Based on the present study, the following conclusions and recommendations have been made:

(i) The analytical expression for the solar cell temperature and electrical efficiency of the photovoltaic thermal (PVT) roof façade of GiSPVT was derived in terms of design and climatic parameters, which is applicable to all weather conditions.

(ii) The performance of energy matrices of various solar cell materials was assessed to determine their suitability for different types of greenhouses, namely low-cost, medium-tech and high-tech greenhouses.

(iii) The comparison among various solar cells material was made for EPBT, EPF, and LCCE on the basis of annual thermal energy (first law of thermodynamics) and exergy (second law of thermodynamics).

(iv) The mc-Si semitransparent PV module was the most suitable choice among the considered solar cell materials for the high-tech GiSPVT system, owing to its longer lifespan and higher life cycle conversion efficiency .

(v) The CIGS was most suitable for low-cost greenhouses.

(vi) It is recommended that the experimental validation of the present thermal model be carried out by considering different solar cell materials for low-cost as well as high-tech uneven greenhouses.

ACKNOWLEDGEMENT

The authors want to extend a sincere thanks to the SODHA ENERGY RESEARCH PARK (SERP), Magupur, Chilkhar, Ballia (India) for this paper.

NOMENCLATURE

A_i	Glass walls/ north roof area (m^2); i=1 (east wall), 2 (south wall), 3 (west wall), 4 (north wall) and 5 (north roof)
A_j	Glass walls area (m^2); j=1 (east wall), 2 (south wall) and 3 (west wall),
A_k	The water pond walls area (m^2); 1(east wall), 2 (south wall), 3 (west wall), 4 (north wall) and 5 (base of water pond)
A_{RS}	Area of south semi-transparent PV module roof (m^2)'
A_w	The water surface area (m^2)
C_w	Specific heat of water, (J/kg°C)
h_1	Total heat transfer coefficient from water surface of pond to Un-even CE greenhouse room air (W/m^2°C)
I(t)	Solar radiation received by south semi-transparent PV module roof (W/m^2)
I_j	Solar radiation received by glass walls (W/m^2); j=1(east wall), 2 (south wall) and 3 (west wall)
M_w	Mass of water in the pond below un-even CE greenhouse (kg)
$\dot{Q}_u$	The hourly thermal energy of water pond (W/m^2)
T_a	Ambient air temperature (°C)
T_c	Solar cell temperature (°C)
T_r	Un-even CE greenhouse room air temperature (°C)
T_w	The temperature of water in pond (°C)
$U_{b,cr}$	An overall bottom heat transfer coefficient from back of solar cell to un-even CE greenhouse room air through glass cover (W/m^2°C)
U_i	An overall bottom heat transfer coefficient from un-even CE greenhouse room air to ambient air temperature through window glass cover (W/m^2°C)
U_k	An overall bottom heat transfer coefficient from water pond of un-even CE greenhouse room to ground temperature through RCC walls/base of pond (W/m^2°C)
U_{Leff}	An overall effective top heat transfer coefficient from water pond of un-even CE greenhouse room to an ambient air temperature through semi-transparent PV roof (W/m^2°C)
$U_{t,ca}$	An overall top heat transfer coefficient from top of solar cell to ambient air temperature through top glass cover of south semi-transparent PV module roof (W/m^2°C)

REFERENCES

1. Agrawal, S.S., & Tiwari, G. N. (2013). Enviroeconomic analysis and energy matrices of glazed hybrid photovoltaic thermal module air collector. Solar Energy, 92, 139-146. https://doi.org/10.1016/j.solener.2013.02.019
2. Declining agricultural land | World Problems & Global Issues. http://encyclopedia.uia.org/en/problems
3. Deo, A., Mishra, G. K., & Tiwari, G. N. (2017). A thermal periodic theory and experimental validation of building integrated semi-transparent photovoltaic thermal (BiSPVT) system. *Solar Energy*, 155, 1021-1032. https://doi.org/10.1016/j.solener.2017.07.013
4. Durisch, W., Bitnar, B., Mayor, J.C., Kiess, H. Lam K., & Close, J. (2007). Efficiency model for PV modules and demonstration of its application to energy yield estimation. *Solar Energy Materials & Solar cells*, 91, 79-84. https://doi.org/10.1016/j.solmat.2006.05.011
5. Evans, D.L. (1981). Simplified method for predicting photo-voltaic output. *Solar Energy*, 27, 555-560. https://doi.org/10.1016/0038-092X(81)90051-7
6. Karthicka, A., Kalidasa K., M., & Kalaivan, L. (2018). Performance analysis of semitransparent photovoltaic module for skylights. *Energy*, 162 (1), 798-812. https://doi.org/10.1016/j.energy.2018.08.043
7. Mishra, R. K., & Tiwari, G. N., (2013). Energy matrices analyses of hybrid photovoltaic thermal (HPVT) water collector with different PV technology. *Solar Energy*, 91, 161-173. https://doi.org/10.1016/j.solener.2013.02.002
8. Murali, M., Basha, H. CH. Hussaian, Kiran, S.R., Akram, P., & Naresh, T. (2021). Performance analysis of different types of solar photovoltaic cell techniques using MATLAB/Simulink. Proceedings of 4th International Conference on Inventive Material Science Applications. *Advances in Sustainability Science and Technology*, Springer, Singapore. https://link.springer.com/chapter/10.1007/978-981-16-4321-7_19
9. Rathore, N., Panwar, N. L. , Yettou, F. & Gama, A., (2019). A comprehensive review of different types of solar photovoltaic cells and their applications. *International Journal of Ambient Energy*, 42 (10), 1200-1217. https://doi.org/10.1080/01430750.2019.1592774
10. Tiwari, G. N., & Mishra, R. K., (2011). Advanced Renewable Energy Sources. Royal Society of Chemistry, UK, 2011. https://books.google.co.in/books/about/Advanced_Renewable_Energy_Sources.html?id=s8gng2vA_88C
11. Tiwari, G. N., (2003). Greenhouse Technology for Controlled Environment, Alpha Science (UK), 2003. https://books.google.co.in/books/about/Greenhouse_Technology_for_Controlled_Env.html?id=K5LVrc6k4WIC&redir_esc=y
12. Tiwari, G. N., Singh, S., Singh, Y. K., & Singh, R. K., (2022). An overall exergy analysis of un-even greenhouse integrated semi-transparent photovoltaic (un-even GiSPVT) system: a thermal modelling approach. International Journal of Ambient Energy, 10.1080/01430750.2022.2050813. https://doi.org/10.1080/01430750.2022.2050813
13. Tiwari, G. N., Singh, S., Singh, Y., Tiwari, A., & Panda, S. K. (Oct. 2022). Enhancement of daily and monthly electrical power of off-grid greenhouse integrated semi-transparent photo-voltaic thermal (GiSPVT) system by integrating earth air heat exchanger (EAHE). *e-Prime Advances in Electrical Engineering, Electronics and Energy*. https://www.sciencedirect.com/science/article/pii/S2772671122000468
14. Tiwari, G.N., & Tiwari, A., (2021). Optimization of packing factor for maximum electric power and crop yield in greenhouse integrated semi-transparent photo-voltaic thermal (GiSPVT) system in desert land: An experimental study. *e-Prime - Advances in Electrical Engineering, Electronics and Energy*, 1, 100008. https://doi.org/10.1016/j.prime.2021.100008
15. Virtuani, A., Pavanello, D., & Friesen, G., (2010). Overview of Temperature coefficients of different thin film photovoltaic technologies. 25th European Photovoltaic Solar Energy Conference and Exhibition / 5th World Conference on Photovoltaic Energy Conversion, Valencia, Spain. https://www.researchgate.net/publication/256080289_Overview_of_Temperature_Coefficients_of_Different_Thin_Film_Photovoltaic_Technologies
16. World population 2022 | Population clock live – Country meters. https://countrymeters.info/en/World
17. Yadav, S. , Panda, S.K., Tiwari, G.N., Helal, Ib., M.A., & Vermette, C.H.. (2022). Periodic theory of greenhouse integrated semi-transparent photovoltaic thermal (GiSPVT) system integrated with earth air heat exchanger (EAHE). Renewable Energy, 184, 45-55. https://doi.org/10.1016/j.renene.2021.11.063